

AC

BCCNT 96/111/258

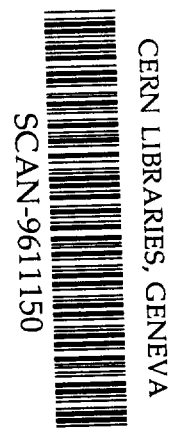
Utility of the Linear Sigma Model for
Scalar Mesons with Spacelike Momenta

L.S. Celenza, Xiang-Dong Li, C.M. Shakin, and Wei-Dong Sun

Department of Physics and Center for Nuclear Theory
Brooklyn College of the City University of New York
Brooklyn, New York 11210

(November, 1996)

Submitted to Physical Review C (Subnucleon Aspects of Nuclei/Physics of Hadrons)



SW 9648

Abstract

We provide evidence for the utility of the linear sigma model in the calculation of the properties of nuclear matter and in the description of nucleon-nucleon scattering. In such studies, the mesons exchanged between nucleons have spacelike momenta. In our model, we show that the dynamics for spacelike momenta of scalar mesons is different than the dynamics in the timelike region (where the nonlinear sigma model is the model of choice). We also show that the interpretation of salient features of relativistic nuclear structure physics is particularly straightforward, if the linear sigma model is used. In our analysis, the properties of scalar-isoscalar exchange between quarks is calculated using the Nambu–Jona-Lasinio (NJL) model for spacelike momenta ($q^2 \leq 0$). In this case, the amplitude behaves as if there was a low-mass sigma meson of mass $m_\sigma \approx 540$ MeV present. For the characterization of the behavior for timelike values of q^2 , we make use of a recent analysis of Törnqvist and Roos that yields a mass for the (physical) sigma meson of 860 MeV with a large width of 880 MeV. It is shown in our work that such mass and width parameters for the sigma meson are consistent with our extended NJL model, which includes a model of confinement. (It is important to note that the pole of the T matrix in the timelike region does not control the behavior in the spacelike region, where the effective sigma mass is found to be 540 MeV.)

I. Introduction

This work is motivated in part by recent work of Furnstahl, Serot, and Tang [1] and of Törnqvist and Roos [2]. The authors of the first of these works have introduced a chiral Lagrangian for use in the calculation of the properties of finite nuclei and of nuclear matter. (Indeed, there has been a good deal of interest in recent years in applying chiral symmetry constraints in the study of nucleon-nucleon scattering [3], as well as many other processes [4].) The authors of Ref. [1] base their work on the nonlinear sigma model and also add rho and omega fields to their Lagrangian. They fit a good deal of data in a model with a number of parameters. However, of most interest to us is the fact that they have to also include a low-mass scalar (sigma) meson to provide the intermediate range attraction in the nucleon-nucleon force. We suggest that the results of Ref. [1] imply that the linear sigma model may be relevant to the study of finite nuclei and nuclear matter. Whether the linear or nonlinear sigma model is appropriate depends upon the underlying dynamics. We will use the Nambu–Jona-Lasinio model, as developed for quark degrees of freedom, to discuss this question. (It has been shown that the NJL model provides a useful low-energy Lagrangian that is consistent with low-energy QCD and chiral perturbation theory.)

It is important to note that, when studying nuclei, nuclear matter, or nucleon-nucleon scattering, the exchanged mesons have spacelike momenta. We wish to argue that, while the nonlinear sigma model is more appropriate for the study of mesons with timelike momenta, there are significant advantages in using the linear sigma model for the study of mesons with spacelike momenta. To support this suggestion, we discuss scalar-isoscalar exchange between quarks, for both spacelike and timelike momenta. We will see that the exchanged "sigma meson" can have

a quite different "mass" in the spacelike and timelike domains. (In the timelike region one does have a pole in the T matrix at rather high energy, while in the spacelike region one has an effective mass of about 540 Mev.)

Some important evidence concerning the nature of the sigma in the timelike region ($q^2 > 0$) is to be found in Ref. [2]. The authors of that work make use of a unitarized quark model that contains six parameters. They describe scalar mesons such as $f_0(980)$, $f_0(1300)$, $K_0^*(1430)$, $a_0(980)$ and $a_0(1450)$ and also fit phase shift data in the case that such data is available. Most important for us, however, is that they find evidence for a scalar-isoscalar resonance that they identify as the long-sought sigma meson. The Breit-Wigner parameters of this resonance are given as $m_{BW} = 860$ MeV and $\Gamma_{BW} = 880$ MeV. We see that the resonance is very broad, as one might infer from the study of the pion-pion phase shift $\delta_0^0(I=0, T=0)$. The results of Ref. [2] are in accord with comments we have made in the past, where we have conjectured that the confining interaction and strong coupling to multipion channels moves the low-mass sigma, predicted by the Nambu–Jona-Lasinio (NJL) model [5], from about 540 MeV to higher energy. [Note that in the SU(2)-flavor NJL model, without confinement, one has $m_\sigma^2 = (2m_q)^2 + m_\pi^2$, where m_q is the constituent quark mass. We have used $m_q = 260$ MeV in our studies of the NJL model.] In this work, we will present a model that has $m_\sigma = 540$ MeV as the (effective) value of the sigma mass in the spacelike region, while the physical state has a significantly higher energy and a large width.

The plan of our work is as follows. In Section II we review some aspects of the NJL model and the results of bosonization. In Section III we describe the calculation of a quark-quark T matrix that may be defined for confined quarks. For spacelike q^2 , we calculate the T

matrix using the NJL model and, for timelike q^2 , we make use of the information obtained by Törnqvist and Roos [2]. We also demonstrate that the NJL model, extended to include a model of confinement, predicts that the sigma meson has an energy and width close to that found in Ref. [2].

In Section IV we consider the interpretation of the large scalar fields found in the Walecka model [6] and in relativistic Brueckner-Hartree-Fock theory [7]. In Section V we discuss the relation of the sigma field to studies of QCD sum rules in matter. In Section VI, we discuss scalar-isoscalar exchange in the nucleon-nucleon interaction and show that our model can reproduce the momentum-transfer dependence of the potential determined in applications of the one-boson-exchange model of the NN force. Information gained in Section VI is used in Section VII to provide a very good, parameter-free fit to the q^2 dependence of the scalar form factor of the nucleon. Finally, in Section VIII, we provide some comments concerning the nonlinear sigma model and present some conclusions.

II. Review of an Extended NJL Model

We may write the Lagrangian for a SU(2)-flavor (extended) NJL model for quarks as

$$\mathcal{L} = \bar{q}(x)(i\partial - m_q^0)q(x) + \frac{G_S}{2}[(\bar{q}(x)q(x))^2 + (\bar{q}(x)i\gamma_5\bar{\tau}q(x))^2] + \mathcal{L}_{conf} \quad , \quad (2.1)$$

where \mathcal{L}_{conf} denotes the contribution to the Lagrangian of the confining interaction, which is essentially a linear potential in our model. (Since our calculations are made in momentum space, we use the Fourier transform of the potential $V^C(r) = \kappa r \exp[-\mu r]$, where $\mu \simeq 0.050$ GeV is used to soften the momentum-space singularities of the Fourier transform of $V^C(r)$.) In the past we have used Lorentz-scalar confinement, with

$$\mathcal{L}_{conf} = \bar{q}(x)q(x)V^C(x-y)\bar{q}(y)q(y) \quad . \quad (2.2)$$

However, in this work we will mainly quote results for Lorentz-vector confinement, where

$$\mathcal{L}_{conf} = \bar{q}(x)\gamma^\mu q(x)V^C(x-y)\bar{q}(y)\gamma_\mu q(y) \quad . \quad (2.3)$$

If we study the dynamical equations for the self-energy of the quark and other quantities, we see that we can relate the κ values appropriate to either Eq. (2.2) or Eq. (2.3). We find $\kappa_{vector} \simeq \kappa_{scalar}/4$ and, since one usually quotes values for κ_{scalar} , we will write the value for κ_{vector} as $\kappa_{vector} = 0.20/4$ GeV², for example, in this work.

In the case of Lorentz-vector confinement, the Lagrangian has chiral symmetry, if the current quark mass, m_q^0 , is zero. In the chiral limit, we find the pion as the massless Goldstone boson. It is often useful to introduce a bosonization procedure [5]. That may be done either by introducing the fields

$$\sigma(x) = -(G_S/g)\bar{q}(x)q(x) \quad (2.4)$$

and

$$\bar{\pi}(x) = -(G_S/g)\bar{q}(x)i\gamma_5\pi q(x) \quad (2.5)$$

as described in Ref. [5], or one may use the elegant momentum-space bosonization procedure of Bernard, Osipov and Meissner [8]. In the absence of confinement, either bosonization procedure shows that there is a sigma meson with $m_\sigma^2 = (2m_q)^2 + m_\pi^2$, where m_q is the constituent quark mass. In most of our work we have adjusted G_S so that $m_q = 260$ MeV. We will continue to use that value of m_q here. Therefore, we find $m_\sigma = 540$ MeV, which is quite close to the value used in the one-boson-exchange (OBE) model of the nucleon-nucleon force [9] or in the Walecka model [6], for example.

The sigma mass may also be determined by studying the quark-quark scattering amplitude. To carry out such a study, we need to define several integrals. For example, the value of the quark-antiquark loop integral (polarization diagram) may be defined in the scalar-isoscalar channel to be

$$-iJ_S(q^2) = (-1)n_f n_c \int \frac{d^4k}{(2\pi)^4} \text{Tr} [iS(k+q/2)iS(k-q/2)] \quad , \quad (2.6)$$

where $n_f=2$ arises from the isospin trace and $n_c=3$ is the number of colors. Further, $S(k) = [k - m_q + i\epsilon]^{-1}$. We have also defined a vertex, $\Gamma_S(q, k)$, that sums a ladder of confining interactions [10]. [See Fig. 1.] Therefore, when we include the effects of confinement, we modify Eq. (2.6) to read

$$-i\hat{J}_S(q^2) = n_c n_f \int \frac{d^4 k}{(2\pi)^4} \text{Tr}[S(k+q/2)\Gamma_S(q,k)S(k-q/2)] . \quad (2.7)$$

The vertex is such that $\Gamma_S(q,k) = 0$ when both the quark and the antiquark go on mass shell [10]. Thus, while $J_S(q^2)$ has unitarity cuts, $\hat{J}_S(q^2)$ is a real function (without cuts).

In Fig. 1, we also show a function, $K_S(q^2)$, that describes the coupling of the $q\bar{q}$ states to the two-pion continuum. Again, introducing confinement, we define $\hat{K}_S(q^2)$ [see Fig. 1e]. Note that $\hat{K}_S(q^2)$ only has cuts when the two pions in the figure go on mass shell.

In Fig. 2 we show some values of $J_S(q^2)$ and $\hat{J}_S(q^2)$ calculated previously. Since confinement is rather unimportant for spacelike q^2 , we only show $J_S(q^2)$ for $q^2 < 0$. The dashed line shows $J_S(q^2)$ in the timelike region. (Note that $\hat{J}_S(q^2) < J_S(q^2)$ in the timelike region.) The sigma mass, in the absence of both confinement and coupling to the two-pion continuum, is found via the solution of the equation

$$G_S^{-1} - J_S(m_\sigma^2) = 0 . \quad (2.8)$$

If we include confinement, we obtain the solid curve for $q^2 > 0$ that represents $\hat{J}_S(q^2)$. If we keep G_S^{-1} fixed, we find a higher value for m_σ when solving the equation

$$G_S^{-1} - \hat{J}_S(m_\sigma^2) = 0 . \quad (2.9)$$

The situation is a bit more complicated than indicated in Eq. (2.9), since the value of G_S is changed somewhat when we introduce confinement [11]. Also, in a more detailed calculation, we should include coupling to the two-pion continuum, so that the equation to determine m_σ becomes

$$G_S^{-1} - \left[\hat{J}_S(m_\sigma^2) + \text{Re } \hat{K}_S(m_\sigma^2) \right] = 0 \quad . \quad (2.10)$$

We have recently determined $\hat{J}_S(q^2)$ and $\hat{K}_S(q^2)$ for Lorentz-vector confinement, which is the model we now prefer [11]. Our calculation of $\text{Re } \hat{K}_S(q^2)$ and $\text{Im } \hat{K}_S(q^2)$ for Lorentz-vector confinement makes use of the methods outlined in Ref. [12]. The values obtained for $\text{Im } \hat{K}_S(q^2)$, which are quite insensitive to the model of confinement used, are given in Fig. 3.

III. The Quark-Quark T Matrix: Scalar-Isoscalar Exchange

The form taken by the quark-quark T matrix, when we consider scalar-isoscalar exchange, has its origin in the various processes shown in Fig. 4. We may sum those diagrams to write, for $q^2 < 0$

$$t_{qq}(q^2) = - \frac{G_S}{1 - G_S[\hat{J}_S(q^2) + \hat{K}_S(q^2)]} . \quad (3.1)$$

In some calculations we may wish to use $\hat{J}_S(q^2) \simeq J_S(q^2)$ and $\hat{K}_S(q^2) \simeq K_S(q^2)$ in the spacelike region, since confinement is a relatively small effect for $q^2 \leq 0$.

In Fig. 5 we show $t_{qq}(q^2)$ of Eq. (3.1) for $q^2 < 0$, with $G_S = 7.91 \text{ GeV}^{-2}$ and $m_q = 260 \text{ MeV}$. Again, with reference to spacelike values of q^2 , we find it useful to define a momentum dependent coupling parameter, $g_{\sigma qq}(q^2)$, such that, for $q^2 \leq 0$,

$$- \frac{G_S}{1 - G_S[\hat{J}_S(q^2) + \hat{K}_S(q^2)]} = \frac{g_{\sigma qq}^2(q^2)}{q^2 - m_\sigma^2} . \quad (3.2)$$

It is then important to note that the behavior of the T matrix in a limited region of spacelike q^2 ($-0.25 \text{ GeV}^2 \leq q^2 \leq 0$) is fit quite well, if we use a constant value for $g_{\sigma qq}(q^2)$. Thus, we have

$$t_{qq}(q^2) = \frac{g_{\sigma qq}^2}{q^2 - m_\sigma^2} , \quad (3.3)$$

where $m_\sigma = 540 \text{ MeV}$ and $g_{\sigma qq} = 3.05$. This value of $g_{\sigma qq}$ was obtained in our earlier work using the relation

$$\frac{G_S}{1 - G_S[\hat{J}_S(0) + \hat{K}_S(0)]} = \frac{g_{\sigma qq}^2}{m_\sigma^2}, \quad (3.4)$$

with $G_S = 7.91 \text{ GeV}^{-2}$, $\hat{J}_S(0) = 0.0826 \text{ GeV}^2$ and $\hat{K}_S(0) = 0.0125 \text{ GeV}^2$. (If we neglect $\hat{K}_S(0)$, we find $g_{\sigma qq} = 2.58$.) The values of $t_{qq}(q^2)$ obtained from Eq. (3.3) are shown as a dotted line in the figure.

In the study of nuclear matter and nucleon-nucleon scattering only relatively small spacelike values of q^2 are needed. Therefore, the parametrization given in Eq. (3.3) is quite useful. We also see that, for small spacelike q^2 , the theory behaves exactly as if there was a pole at $q^2 = m_\sigma^2$ with $m_\sigma \cong 540 \text{ MeV}$. However, as we will see, there is no such low-energy pole in the timelike region.

Before we go on to consider the timelike region, we may note that a similar conclusion concerning an effective mass for scalar-isoscalar exchange for $q^2 \leq 0$ may be found from our study of hadronic correlation functions [12]. For example, we may define a scalar-isoscalar current, $j_S(x) = \bar{q}(x)q(x)$, and a correlation function

$$iC(q^2) = \int d^4x e^{iq \cdot x} \langle 0 | T(j(x)j(0)) | 0 \rangle. \quad (3.5)$$

We have solved for $C(q^2)$ via a dispersion relation [12]

$$C(q^2) = \hat{J}_S(q^2) - \frac{1}{\pi} \int_{4m_\pi^2}^{\infty} \frac{\text{Im} C(q'^2)}{q^2 - q'^2 + i\epsilon}, \quad (3.6)$$

where $\hat{J}_S(q^2)$ is real. (In practice, the upper limit for the integral is about $q^2 = 1 \text{ GeV}^2$.) In Fig. 6, we show the correlation function calculated in Ref. [12]. In the figure, the dotted line represents the approximation

$$\text{Re}C(q^2) + \hat{J}_S(q^2) = \frac{f_\sigma^2 m_\sigma^2}{q^2 - m_\sigma^2} , \quad (3.7)$$

where, in making a fit to the solid line, we have used $m_\sigma = 540$ MeV. (Here, f_σ is a sigma decay constant.) Note the excellent fit of the dotted line to the curve for $t = q^2 < 0$. Also, we see that there is no pole at $t = m_\sigma^2$. Therefore, we again see that the effective value of the mass in the spacelike region ($t < 0$) is $m_\sigma = 540$ MeV, even though there is no physical particle with that mass. The results of the calculation presented in Fig. 6 should be improved. A better calculation of $\text{Im} \hat{K}_S(q^2)$ is needed and vector confinement should be used, rather than the scalar confinement used in Ref. [12]. However, the improved calculation will exhibit the feature we stress. That is, the behavior in the spacelike region will be parametrized by Eq. (3.7), with $m_\sigma = 540$ MeV.

We now return to a consideration of the T matrix. Values of $t_{qq}(q^2)$ were given in Fig. 5 for $q^2 < 0$, making use of Eq. (3.1). For the timelike region, we write

$$t_{qq}(q^2) = \frac{\hat{g}_{\sigma qq}^2(q^2)}{q^2 - \bar{m}_\sigma^2 + i\bar{m}_\sigma \Gamma_\sigma(q^2)} \quad (3.8)$$

and use the results of Ref. [2] for \bar{m}_σ and Γ_σ . Thus, we put $\bar{m}_\sigma = 860$ MeV and $\Gamma_\sigma(\bar{m}_\sigma^2) = 880$ MeV. Thus,

$$\Gamma_\sigma(q^2) = \left[1 - \frac{4m_\pi^2}{q^2} \right]^{1/2} \hat{\Gamma}_\sigma , \quad (3.9)$$

with $\hat{\Gamma}_\sigma = 929$ MeV [2]. The value of $\hat{g}_{\sigma qq}^2 = 23.6$ makes for a continuous representation of $\text{Re} t_{qq}(q^2)$ in Fig. 5, as we pass from the spacelike to the timelike region. Note also that

$\tilde{g}_{\sigma qq} > g_{\sigma qq}$, since we use a different mass to parametrize the T matrix for the $q^2 < 0$ and the $q^2 > 0$ regions. With our parametrization, we have

$$\frac{\tilde{g}_{\sigma qq}^2}{\tilde{m}_\sigma^2} = \frac{g_{\sigma qq}^2}{m_\sigma^2} \quad (3.10)$$

so that, with $g_{\sigma qq} = 3.05$, $m_\sigma = 0.540$ GeV and $\tilde{m}_\sigma = 0.860$ GeV, we find $\tilde{g}_{\sigma qq}^2 = 23.6$. The change in the parameters when passing from the spacelike to the timelike region could be avoided by using a "running" mass parameter, $m_\sigma(q^2)$, that would vary continuously from 540 MeV for $q^2 = 0$ to 860 MeV when $q^2 = (0.860 \text{ GeV})^2$. (Note, however, that with our parametrization, we may still construct a continuous quark-quark T matrix as seen in Fig. 5.) The T matrix of Fig. 5 has the behavior calculated with the NJL model for $q^2 < 0$ and for $q^2 > 0$ it is accordance with the Breit-Wigner parametrization of Ref. [2]. We may now check whether the large width of 880 MeV is consistent with the NJL model. The width is related to $\text{Im } \hat{K}_S(q^2)$ given in Fig. 3,

$$\Gamma_\sigma(\tilde{m}_\sigma^2) = \frac{\tilde{g}_{\sigma qq}^2}{\tilde{m}_\sigma} \text{Im } \hat{K}_S(\tilde{m}_\sigma^2) \quad (3.11)$$

With $\tilde{g}_{\sigma qq}^2 = 23.6$, $\tilde{m}_\sigma = 0.860$ GeV, $g_{\pi qq} = 2.68$, and $\text{Im } \hat{K}_S(\tilde{m}_\sigma^2) = 0.037 \text{ GeV}^2$, we find $\Gamma_\sigma = 1015$ MeV. That value is not far from the value $\Gamma_\sigma = 880$ MeV, suggested in Ref. [2]. The result indicates that quite large widths are to be expected when using the NJL model. It is also useful to note that as we pass from the spacelike to the timelike region of q^2 , with $q^2 > 4m_\pi^2$, the width of any scalar-isoscalar excitation we calculate would quite rapidly become large.

We now consider the mass of the physical sigma meson. For simplicity, we neglect

Re $\hat{K}_S(q^2)$ and study

$$G_S^{-1} - \hat{J}_S(\tilde{m}_\sigma^2) = 0 \quad . \quad (3.12)$$

We make use of Lorentz-vector confinement for this study. We proceed by calculating the quark self-energy, $\Sigma(k) = A(k^2) + \not{k}B(k^2)$, where we now include the confining interaction, in addition to the NJL interaction [11]. That leads to a relatively small k^2 dependence of $A(k^2)$ and $B(k^2)$. We then adjust G_S so that $A(0) = m_q$, with $m_q = 260$ MeV, as used previously. Thus, for $\kappa = 0.20/4$ GeV², we find $G_S = 8.516$ GeV⁻² [11]. Using vector confinement, we find the values of $\hat{J}_S(q^2)$ shown in Fig. 7. A horizontal line representing G_S^{-1} provides a graphical solution of Eq. (3.12). In this fashion, we find $\tilde{m}_\sigma = 800$ MeV which is reasonably close to the value of $\tilde{m}_\sigma = 860$ MeV determined in Ref. [2].

IV. Lorentz-Scalar Potentials of Relativistic Nuclear Physics

Some years ago we discussed the idea that the large scalar fields in nuclei were related to a partial restoration of chiral symmetry at finite baryon density [13]. To carry out that discussion we made use of the linear sigma model with the sigmas and pions coupled to the nucleon. Developments since that time allow for a more informed discussion. For example, there is a useful model-independent relation due to Drukarev and Levin [14], that relates the reduction in the value of the quark condensate in matter to the pion nucleon sigma term, σ_N ,

$$\langle \psi | \bar{q}q | \psi \rangle = \langle 0 | \bar{q}q | 0 \rangle \left[1 - \frac{\sigma_N \rho}{m_\pi^2 f_\pi^2} \right]. \quad (4.1)$$

Here, ρ is the baryon density and f_π is the pion decay constant. With $\rho \simeq (0.109 \text{ GeV})^3$ and $\sigma_N = 45 \text{ MeV}$, Eq. (4.1) implies a 35 percent reduction of the condensate in nuclear matter.

In the bosonization scheme discussed earlier, it is easy to see that the sigma field has the value f_π in vacuum and that it is proportional to the value of the quark condensate. Thus from Eq. (4.1), we have

$$\sigma = f_\pi \left[1 - \frac{\sigma_N \rho}{m_\pi^2 f_\pi^2} \right]. \quad (4.2)$$

It is useful to define $\sigma = f_\pi + \sigma'$. Then,

$$\sigma' = - \frac{\sigma_N \rho}{m_\pi^2 f_\pi} \quad (4.3)$$

is the value of the fluctuation field, with $\sigma' = -35 \text{ MeV}$ in nuclear matter. It is then of interest to note that -35 MeV is close to the value of the Lorentz scalar field in nuclear matter in the Walecka model [6] or in relativistic Brueckner-Hartree-Fock theory [7]. In the simplest

formulation, the scalar field in nuclear matter is given by

$$V_\sigma = - \frac{G_{\sigma NN}^2}{m_\sigma^2} . \quad (4.4)$$

The sigma-nucleon coupling constant, $G_{\sigma NN}$, has a value of about 9.5 [9] so that $V_\sigma \simeq -400$ MeV. The value chosen for $G_{\sigma NN}$ is somewhat model dependent, however, simple estimates give $G_{\sigma NN} \sim 9$. For example, the sigma nucleon coupling constant can be calculated as $G_{\sigma NN} = g_{\sigma qq}(0) F_S^{val}(0)$, where $F_S^{val}(q^2)$ is the scalar form factor of the valence quarks in the nucleon [15]. Such a valence form factor has been calculated as part of a lattice simulation of QCD, where the scalar form factor of the nucleon is calculated [16]. It was found in Ref. [16] that $F_S^{val}(0) = 3.02$, so that with $g_{\sigma qq}(0) = 3.05$, as used earlier in this work, we have $G_{\sigma NN} = 9.21$.

V. Scalar Fields and QCD Sum Rules in Matter

In the simplest analysis of QCD sum rules in matter, one derives a relation between the nucleon mass in matter, m_N^* , and the condensate in matter $\langle \bar{u}u + \bar{d}d \rangle_\rho$, where u and d stand for the fields of the up and down quarks [17]. The expression for the self-energy is given in terms of the Borel mass, M ,

$$\Sigma_S = - \frac{8\pi^2}{M^2} \frac{\langle \bar{u}u + \bar{d}d \rangle_\rho}{2} \quad (5.1)$$

where the subscript ρ indicates the presence of nuclear matter. In vacuum, $\Sigma_S = m_N$, with

$$m_N = - \frac{8\pi^2}{M^2} \frac{\langle \bar{u}u + \bar{d}d \rangle_0}{2} \quad (5.2)$$

where the zero subscript denotes the vacuum value. With $M=1.18$ GeV and $\langle \bar{u}u \rangle_0 = \langle \bar{d}d \rangle_0 = (-0.254 \text{ GeV})^3$, one finds $m_N = 930$ MeV.

In the following discussion we will assume the current quark mass is zero and we will also neglect $\hat{K}_S(q^2)$, the function that describes the coupling of the quark-antiquark states to the two-pion continuum. Therefore, with $m_q^0 = 0$, we have

$$m_q = - G_S \langle \bar{u}u + \bar{d}d \rangle_0 \quad (5.3)$$

in the NJL model. With $G_S = 7.91 \text{ GeV}^{-2}$ and $\langle \bar{u}u \rangle_0 = (-0.254 \text{ GeV})^3$, we get $m_q = 260$ MeV, for example.

We can insert the relation used in a bosonization scheme,

$$\sigma = - \frac{G_S}{g_{\sigma qq}} \langle \bar{u}u + \bar{d}d \rangle_\rho, \quad (5.4)$$

in Eq. (5.1) to get [18]

$$\Sigma_S = \frac{8\pi^2}{M^2} \frac{g_{\sigma qq}}{2G_S} \sigma . \quad (5.5)$$

We use $\sigma = f_\pi + \sigma'$, so that

$$\Sigma_S = \frac{8\pi^2}{M^2} \frac{g_{\sigma qq}}{2G_S} (f_\pi + \sigma') . \quad (5.6)$$

For the work of this section, we have neglected $\hat{K}_S(q^2)$. Therefore $g_{\sigma qq}$ has a smaller value than the value of 3.05 used earlier. We find $g_{\sigma qq} = 2.65$ and with $m_q = 260$ MeV, we then obtain $f_\pi = 0.098$ GeV, upon use of the Goldberg-Treiman relation. The first term on the right-hand side of Eq. (5.6) yields $m_N = 930$ MeV, as given above.

Now let us put $\sigma' = -35$ MeV, as suggested earlier in this work. [See Eq. (4.3).]

Then,

$$\Sigma_S = m_N + \frac{8\pi^2}{M^2} \frac{g_{\sigma qq}}{2G_S} \sigma' \quad (5.7)$$

$$= m_N + V_S . \quad (5.8)$$

We find $V_S = -332$ MeV, which is comparable to the large value of the scalar potential that is used in the Walecka model ($V_s \sim -400$ MeV), for example.

VI. Scalar-Isoscalar Exchange in the Nucleon-Nucleon Force

In this section we review some of our work concerning sigma exchange between nucleons. We will discuss the relation of our model and the one-boson-exchange (OBE) model [9]. In the OBE model, the potential due to sigma exchange depends upon a vertex cutoff at each meson-nucleon vertex, a coupling constant and a meson propagator. Thus,

$$V_{\sigma}^{OBE}(q^2) = g_{\sigma NN}^2 \left[\frac{\Lambda_{OBE}^2 - m_{\sigma}^2}{\Lambda_{OBE}^2 - q^2} \right]^2 \frac{1}{q^2 - m_{\sigma}^2} , \quad (6.1)$$

where we have left out reference to the nucleon spinors and isospinors, for simplicity. Let us define the amplitude $f_{\sigma}^{OBE}(q^2) = V_{\sigma}^{OBE}(q^2)/4\pi$. The corresponding interaction in the NJL model has valence-quark form factors rather than vertex cutoffs. Thus we have

$$f_{\sigma}^{NJL}(q^2) = \frac{t_{qq}(q^2)}{4\pi} [F_{\sigma}^{val}(0)]^2 \left[\frac{\lambda_{\sigma}^2}{\lambda_{\sigma}^2 - q^2} \right]^2 , \quad (6.2)$$

where

$$F_{\sigma}^{val}(q^2) = F_{\sigma}^{val}(0) \left[\frac{\lambda_{\sigma}^2}{\lambda_{\sigma}^2 - q^2} \right] \quad (6.3)$$

is the valence-quark scalar form factor of the nucleon. Equation (6.3) serves to define the parameter λ_{σ} . We also write

$$f_{\sigma}^{OBE}(q^2) = f_{\sigma}^{OBE}(0) h_{\sigma}^{OBE}(q^2) , \quad (6.4)$$

and

$$f_{\sigma}^{NJL}(q^2) = f_{\sigma}^{NJL}(0) h_{\sigma}^{NJL}(q^2) . \quad (6.5)$$

Note that $h_\sigma^{NJL}(0) = h_\sigma^{OBE}(0) = 1$. It is useful to compare $h_\sigma^{NJL}(q^2)$ and $h_\sigma^{OBE}(q^2)$. We choose the parameter λ_σ so that these two functions are similar over a large range of q^2 and find that $\lambda_\sigma = 1.10$ GeV leads to an excellent fit. [See Fig. 8.] Note that, since the exchanged mesons are spacelike ($q^2 \leq 0$), we have used the effective sigma mass in the spacelike region of $m_\sigma = 540$ MeV, when calculating the amplitude for the NJL model.

VII. The Scalar Form Factor of the Nucleon

In the last section, we found a value of $\lambda_\sigma = 1.10$ GeV in our parametrization of the valence-quark form factor of the nucleon. In this section, we show how that information may be used to calculate the scalar form factor of the nucleon $F_S(q^2)$. We define $F_S(q^2)$ using the relation

$$F_S(q^2) u(\bar{\mathbf{p}} + \bar{\mathbf{q}}, s') u(\bar{\mathbf{p}}, s) \delta_{\tau\tau'} = \langle N, \bar{\mathbf{p}} + \bar{\mathbf{q}}, s', \tau' | \bar{q}(0) q(0) | N, \bar{\mathbf{p}}, s, \tau \rangle, \quad (7.1)$$

where the $u(\bar{\mathbf{p}}, s)$ are Dirac spinors, and s and τ are isospin labels. We may use a sigma-dominance model to calculate $F_S(q^2)$. For example, we may sum the diagrams shown in Fig. 9. The first term is the contribution of valence quarks, which we identify with $F_\sigma^{val}(q^2)$ of Eq. (6.3). Summing the various quark-antiquark polarization diagrams shown in Fig. 9, we find

$$F_S(q^2) = \frac{1}{1 - G_S J_S(q^2)} F_\sigma^{val}(q^2). \quad (7.2)$$

We define the amplitude

$$f_S(q^2) = \frac{F_S(q^2)}{F_S(0)}, \quad (7.3)$$

$$= \frac{1 - G_S J_S(0)}{1 - G_S J_S(q^2)} \left[\frac{\lambda_\sigma^2}{\lambda_\sigma^2 - q^2} \right], \quad (7.4)$$

where we have used Eq. (6.3). There are no free parameters at this point. With $\lambda_\sigma = 1.10$ GeV, we compare, in Fig. 10, $f_S(q^2)$ with the corresponding quantity calculated in a lattice simulation of QCD [16]. The fit is quite good, particularly, since there are no adjustable parameters.

We note that we can write

$$f_S(q^2) = \frac{m_\sigma^2}{m_\sigma^2 - q^2} \cdot \frac{g_{\sigma qq}^2(q^2)}{g_{\sigma qq}^2(0)} \cdot \frac{\lambda_\sigma^2}{\lambda_\sigma^2 - q^2} \quad (7.5)$$

where $q^2 \leq 0$. It is interesting to see that the fit shown in Fig. 10 can be considered as resulting from the use of a sigma dominance model. However, one should not neglect the second factor on the right-hand side of Eq. (7.5). Neglect of the q^2 dependence of $g_{\sigma qq}(q^2)$ would result in a less satisfactory fit, even for small q^2 . For example, in Fig. 11 we show the q^2 dependence of $g_{\sigma qq}(q^2)$. (The figure shows $g_{\sigma qq}(s)$, with $s = q^2$.) To calculate $g_{\sigma qq}(q^2)$ for $q^2 < 0$, we have made use of the definition given in Eq. (3.2), and have used the approximation $\hat{J}_S(q^2) \simeq J_S(q^2)$ and $\hat{K}_S(q^2) \simeq K_S(q^2)$.

VIII. Discussion

We were motivated to write this paper because of the results of Ref. [1]. That work represents a comprehensive effort to use modern ideas concerning effective chiral Lagrangians [4] in nuclear structure studies. It was found necessary, however, to include a low-mass scalar field in the Lagrangian of the nonlinear sigma model. (The physical interpretation of that field is unclear.) We recall that the nonlinear sigma model may be related to the linear version by requiring that the sigma and pion fields be constrained to the chiral circle. More precisely, one may write [4]

$$\sigma(x) + i \vec{\pi}(x) \cdot \vec{\tau} = f_{\pi} \exp[i \vec{\pi}'(x) \cdot \vec{\tau}/f_{\pi}] . \quad (8.1)$$

The Lagrangian is then written in terms of the matrix

$$U = \exp[i \vec{\pi}'(x) \cdot \vec{\tau}/f_{\pi}] . \quad (8.2)$$

In this manner, the sigma meson is removed as an independent degree of freedom.

In this work, we have suggested that the constraint implied by Eq. (8.1) is not appropriate for the study of many problems in nuclear physics. We have attempted to demonstrate, using results of the NJL model and some information from Ref. [2], that the "sigma meson" is quite a different object when one looks at spacelike or timelike values of q^2 . At spacelike values of q^2 , the linear sigma model, which may be obtained by bosonization of the NJL model, describes the dynamical situation quite well. The use of that model allows one to make contact with the treatment of QCD sum rules in matter and with relativistic many-body theories such as quantum hadrodynamics (QHD) [6] and Dirac-Brueckner-Hartree-Fock theory [7]. We have also seen that we may understand the intermediate-range attraction in the nucleon-

nucleon force, as well as the scalar form factor of the nucleon using our formalism.

We have found it useful to study the quark-quark interaction in momentum-space using the NJL model. We have usually not performed a bosonization of the standard form. Rather, we have parametrized the quark-quark T matrices in terms of the pole position and width of the resonance. That is a particularly useful procedure in the case of the scalar-isoscalar channel where the characteristics of the T matrix are such as to require a different parametrization for spacelike q^2 and for timelike q^2 . This complexity is probably due to the very strong coupling of the quark-antiquark states to the two-pion continuum, since for other channels governed by pion, rho, or omega exchange, the T matrix may be represented by a single parametrization over the full range of q^2 .

Acknowledgement

This work is supported in part by a grant from the National Science Foundation and by the PSC-CUNY Faculty Research Award Program of the City University of New York.

References

- [1] R.J. Furnstahl, B.D. Serot, Hua-Bin Tang, preprint of Ohio State University, OSU-96-612 (1996); nucl-th/9608035.
- [2] N.A. Törnqvist and M. Roos, Phys. Rev. Lett. 76, 1575 (1996).
- [3] L.S. Celenza, A. Pantziris, and C.M. Shakin, Phys. Rev. C46, 2213 (1992).
C. Ordóñez, L. Ray, and U. van Kolck, Phys. Rev. Lett. 72, 1982 (1994).
C. Ordóñez, L. Ray, and U. van Kolck, Phys. Rev. C53, 2086 (1996).
S. Weinberg, Phys. Lett. B251, 288 (1990).
S. Weinberg, Nucl. Phys. B363, 3 (1991).
D.B. Kaplan, M.J. Savage, and M.B. Wise, Nucleon-Nucleon Scattering from Effective Field Theory preprint: Inst. for Nuclear Theory, Univ. of Washington INT96-00-125 (1996).
- [4] For a good introduction to chiral perturbation theory and the nonlinear sigma model, see J. Donoghue, E. Golowich, and B.R. Holstein, Dynamics of the Standard Model (Cambridge Univ. Press, Cambridge, 1992).
- [5] See, for example, the review of the NJL model in S.P. Klevansky, Rev. Mod. Phys. 64 649 (1992).
- [6] B.D. Serot and J.D. Walecka, in Advances in Nuclear Physics, edited by J.W. Negele and E. Vogt (Plenum, New York, 1986) Vol. 16.
- [7] L.S. Celenza and C.M. Shakin Relativistic Nuclear Physics: Theories of Structure and Scattering (World Scientific, Singapore, 1986).
- [8] V. Bernard, A.A. Osipov, and Ulf.-G. Meissner, Phys. Lett. B285, 119 (1992).

- [9] R. Machleidt, in Advances in Nuclear Physics, edited by J.W. Negele and E. Vogt (Plenum, New York, 1988) Vol. 19.
- [10] L.S. Celenza, C.M. Shakin, Wei-Dong Sun, J. Szweda, and Xiquan Zhu, Phys. Rev. D51, 3638 (1995).
- [11] L.S. Celenza, Xiang-Dong Li, and C.M. Shakin, Brooklyn College Report: BCCNT 96/101/257 (1996).
- [12] L.S. Celenza, C.M. Shakin, Wei-Dong Sun, J. Szweda, and Xiquan Zhu, Intl. J. Mod. Phys. E2, 603 (1993).
- [13] B. Goulard, L.S. Celenza, and C.M. Shakin, Phys. Rev. D24, 912 (1981); see also, L.S. Celenza, A. Pantziris, C.M. Shakin, and Wei-Dong Sun, Phys. Rev. C45, 2015 (1992); *ibid.* C46, 571 (1992).
- [14] E.G. Drukarev and E.M. Levin, Nucl. Phys. A532, 695 (1991); E.G. Drukarev and E.M. Levin, Prog. Part. Nucl. Phys. 27, 77 (1991).
- [15] C.M. Shakin and Wei-Dong Sun, Scalar-Isoscalar Meson Exchange in the Calculation of the Nuclon-Nucleon Interaction, Brooklyn College Report: BCCNT 96/041/255 (1996) - submitted for publication.
- [16] S.J. Dong, J.-F. Lagaë, and K.F. Liu, Univ. of Kentucky preprint: UK 95-12 (1995); hep-ph/9602259.
- [17] T.D. Cohen, R.J. Furnstahl, and D.K. Griegel, Phys. Rev. Lett. 67, 961 (1991).
- [18] C.M. Shakin, Phys. Rev. C50, 1139 (1994).

Figure Captions

- Fig. 1 (a) The zero-range quark interaction of the NJL model is shown.
- (b) The quark-loop integral in the scalar-isoscalar channel is shown.
- (c) The quark-loop integral including a series of confining interactions (dashed line) is shown. The filled triangular region denotes the vertex function that serves to sum the ladder of confining interactions.
- (d) The function $K_S(q^2)$ describes effects of coupling to the two-pion continuum.
- (e) The function $\hat{K}_S(q^2)$ includes two confinement vertex functions and has a cut for $q^2 > 4m_\pi^2$.

Fig. 2 The function $J_S(t)$ is represented by a solid line for $t = q^2 < 0$ and by a dashed line for $t = q^2 > 0$. The calculation of $J_S(t)$ is made by passing to a Euclidean momentum space with $k_E^2 \leq \Lambda_E^2$ ($\Lambda_E = 1.0$ GeV). If we include confinement we obtain $\hat{J}_S(t)$, shown as a solid line for $t \geq 0$. The dotted line serves to interpolate between $J_S(t)$ and $\hat{J}_S(t)$ to yield a continuous curve. These calculations we made with $m_q = 260$ MeV and with a Lorentz-scalar confinement model. For $\hat{J}_S(t)$, and for $t > 0$, the calculation is made in Minkowski space. We find $J_S(0) = 0.0880$ GeV² and $\hat{J}_S(0) = 0.0826$ GeV². [See Fig. 7.]

Fig. 3 Values of $\text{Im } \hat{K}_S(q^2)$ are shown. The calculation is made using the method outlined in Ref. [12]. Here we use $\kappa = 2.0/4$ GeV², $g_{\pi qq} = 2.58$ and Lorentz-vector confinement. We also have $m_q = 260$ MeV and a cutoff on the three-momenta, $|\vec{k}| \leq \Lambda_3$, with $\Lambda_3 = 0.689$ GeV. (Note that the result is quite insensitive to the model of confinement used.)

Fig. 4 The quark-quark T matrix $t_{qq}(q^2)$ is obtained by summing the diagrams shown. The t -channel exchanges are summed by the expression given as Eq. 3.1. In a limited region of q^2 ($-0.25 \text{ GeV}^2 < q^2 < 0$), these effects are well represented by the exchange of an effective sigma meson with $m_\sigma = 540 \text{ MeV}$, as may be seen in Fig. 5.

Fig. 5 Values of $\text{Re } t_{qq}(t)$ and $\text{Im } t_{qq}(t)$ are shown. For $q^2 = t < 0$, the solid line represent the values obtained using Eq. (3.1), with the approximations $\hat{K}_S(q^2) \approx K_S(q^2)$ and $\hat{J}_S(q^2) \approx J_S(q^2)$. The dotted line represents $g_{\sigma qq}^2 / (t - m_\sigma^2)$ with $m_\sigma = 540 \text{ MeV}$ and $g_{\sigma qq} = 3.05$. For $t = q^2 > 0$, we use the parameters of Törnqvist and Roos, $m_\sigma = 860 \text{ MeV}$ and $\Gamma_\sigma = 880 \text{ MeV}$ [2]. (See Eq. 3.8.) For $t > 0$, the solid line is $\text{Re } t_{qq}(t)$ and the dashed line is $\text{Im } t_{qq}(t)$.

Fig. 6 The figure shows the scalar-isoscalar hadronic correlation function calculated in Ref. [12]. The solid line represents $\text{Re } C(t) + \hat{J}_S(t)$ and the dashed line shows $\text{Im } C(t)$. The dotted line represents the function $f_\sigma^2 m_\sigma^2 / (t - m_\sigma^2)$ with $m_\sigma = 540 \text{ MeV}$. (Here, f_σ is the sigma decay constant.) Note that for $q^2 = t < 0$, the correlator is well approximated by a sigma-dominance model. However, there is no corresponding pole in the timelike region. [See caption to Fig. 5.]

Fig. 7 The figure shows $J_S(q^2)$ and $\hat{J}_S(q^2)$ calculated for $q^2 \geq 0$. (We use a cutoff on the three-momenta in the loop integral of $|\vec{k}| \leq \Lambda_3$, with $\Lambda_3 = 0.689 \text{ GeV}$.) The dotted curve is the result in the absence of confinement and the solid line shows $\hat{J}_S(q^2)$ for Lorentz-vector confinement with $\kappa = 0.20/4 \text{ GeV}^2$. For the

dotted curve ($\kappa=0$) we have $G_S = 7.91 \text{ GeV}^{-2}$ and for the solid curve ($\kappa = 0.05 \text{ GeV}^2$) we have $G_S = 8.516 \text{ GeV}^{-2}$. Without confinement we find $m_\sigma = 540 \text{ MeV}$, while, with confinement included, we find $m_\sigma = 800 \text{ MeV}$. The horizontal dashed lines denote G_S^{-1} for the two cases. The intersection of the appropriate dashed line with the dotted or solid lines determines the mass of the sigma. (The dotted curve is the same as the dashed curve of Fig. 2.) Here $J_S(0) = 0.088 \text{ GeV}^2$ and $\hat{J}_S(0) = 0.070 \text{ GeV}^2$.

Fig. 8 The values of $h_\sigma^{OBE}(q^2)$ [dotted line] and $h_\sigma^{NJL}(q^2)$ [solid line] are shown. Here, $\lambda_\sigma = 1.10 \text{ GeV}$. For the OBE amplitude we use $m_\sigma = 550 \text{ MeV}$ and $\Lambda_\sigma = 1.5 \text{ GeV}$ [9].

Fig. 9 Calculation of the scalar form factor of the nucleon. The operator $\bar{q}(0)q(0)$ is denoted by the large filled circle. The single lines represent quarks or antiquarks.

- (a) The valence contribution is shown.
- (b)-(c) A series of quark-antiquark loop diagrams is shown.
- (d) A sigma-dominance model representing the diagrams shown in a, b, c, etc.

There, the small open circle represents $g_{\sigma qq}$.


Fig. 10 The values calculated for $f_S(q^2) = F_S(q^2)/F_S(0)$ are shown. Here $\lambda_\sigma = 1.10 \text{ GeV}$. The circles with the error bars are the results of the QCD lattice simulation of Ref. [16].

Fig. 11 This figure shows $g_{\sigma qq}(s)$ for $s \leq 0$, where $s = q^2$. The q^2 dependence of the coupling constant is needed to provide an accurate representation of the T matrix,

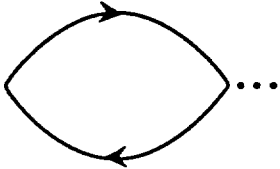
$t_{qq}(q^2)$. For $q^2 < 0$, we have used

$$t_{qq}(q^2) = \frac{g_{\sigma qq}^2(q^2)}{q^2 - m_\sigma^2}$$

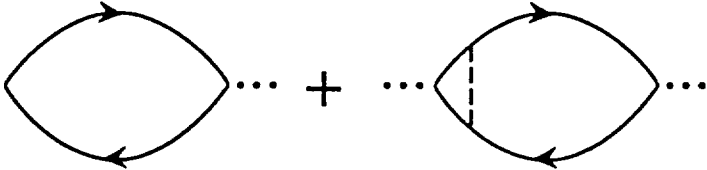
to define $g_{\sigma qq}(q^2)$.

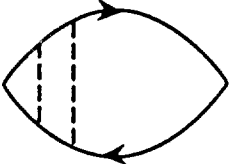
$$iG_S$$


(a)

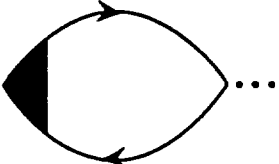
$$-iJ_S(q^2) = \dots$$


(b)

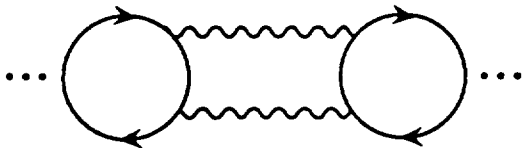
$$-i\hat{J}_S(q^2) = \dots$$


$$+ \dots$$


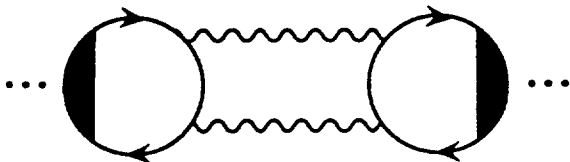
$$+ \dots$$

$$= \dots$$


(c)

$$-iK_S(q^2) = \dots$$


(d)

$$-i\hat{K}_S(q^2) = \dots$$


(e)

FIG. 1

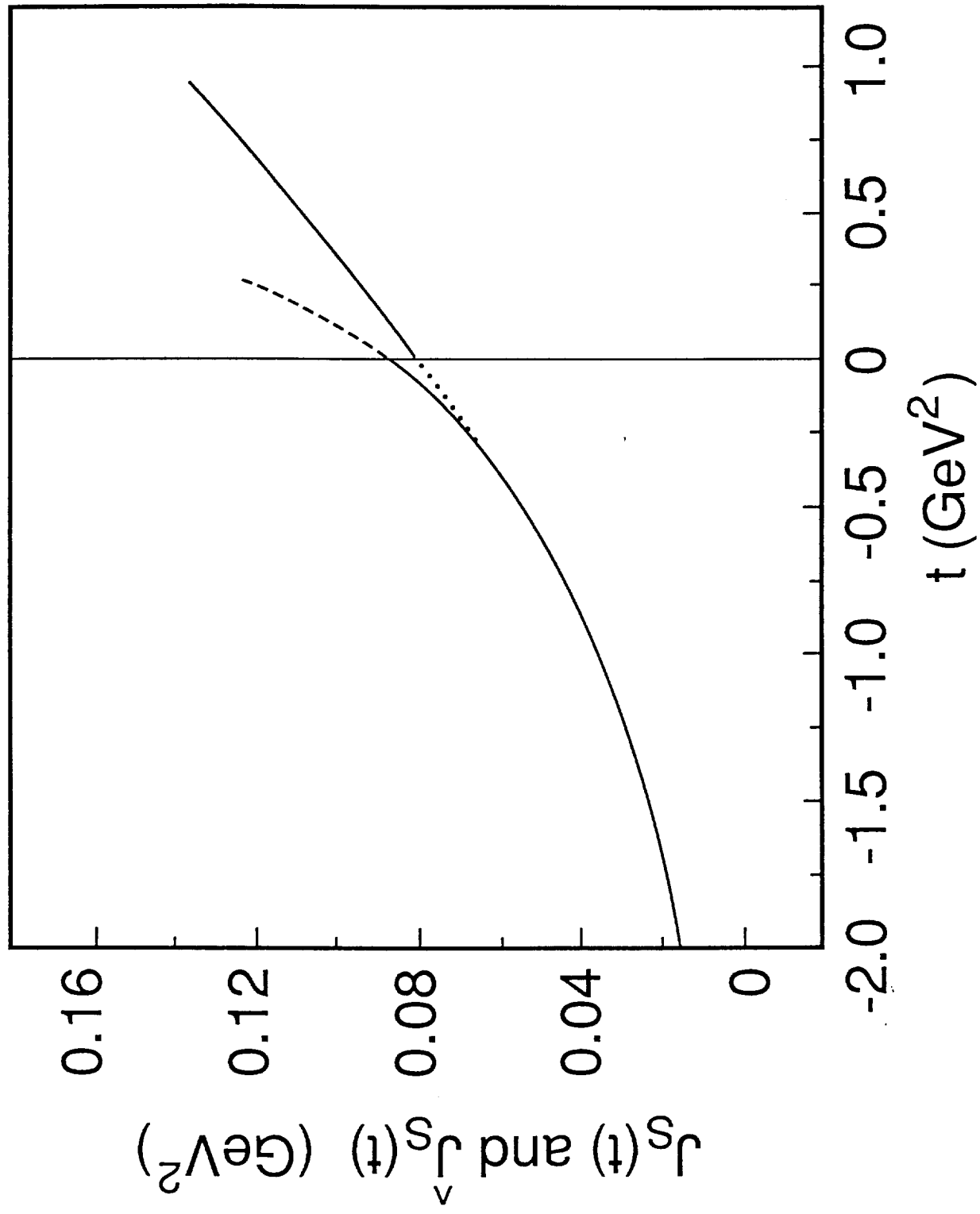


FIG. 2

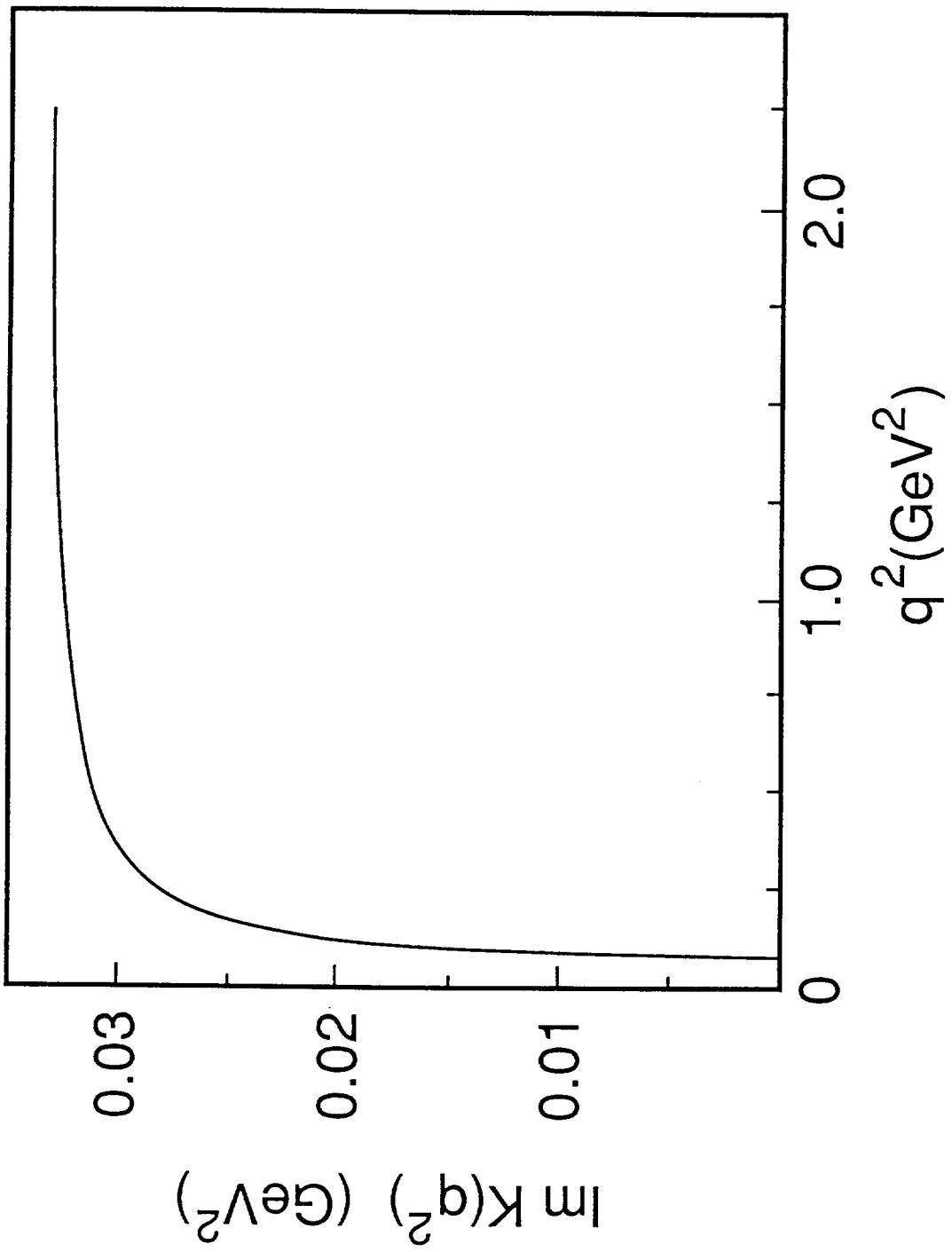


FIG. 3

$$\begin{aligned}
 & -it_{qq}(q^2) = \\
 & \begin{array}{c}
 \text{Diagram 1} \\
 + \\
 \text{Diagram 2}
 \end{array} \\
 & \begin{array}{c}
 \dots \\
 + \\
 \text{Diagram 3} \\
 + \\
 \text{Diagram 4} \\
 + \\
 \text{Diagram 5} \\
 + \\
 \dots
 \end{array}
 \end{aligned}$$

FIG. 7

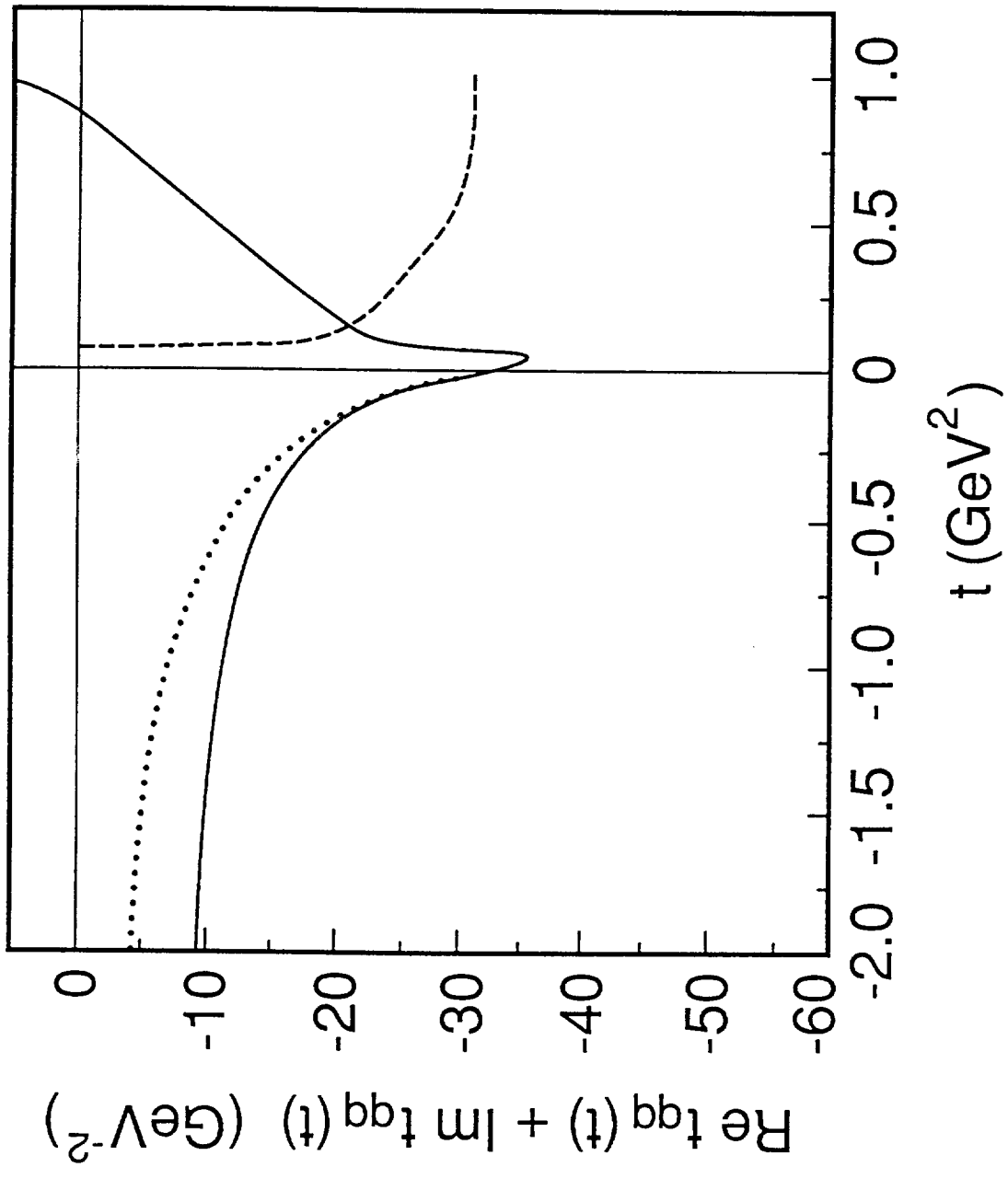


FIG. 5

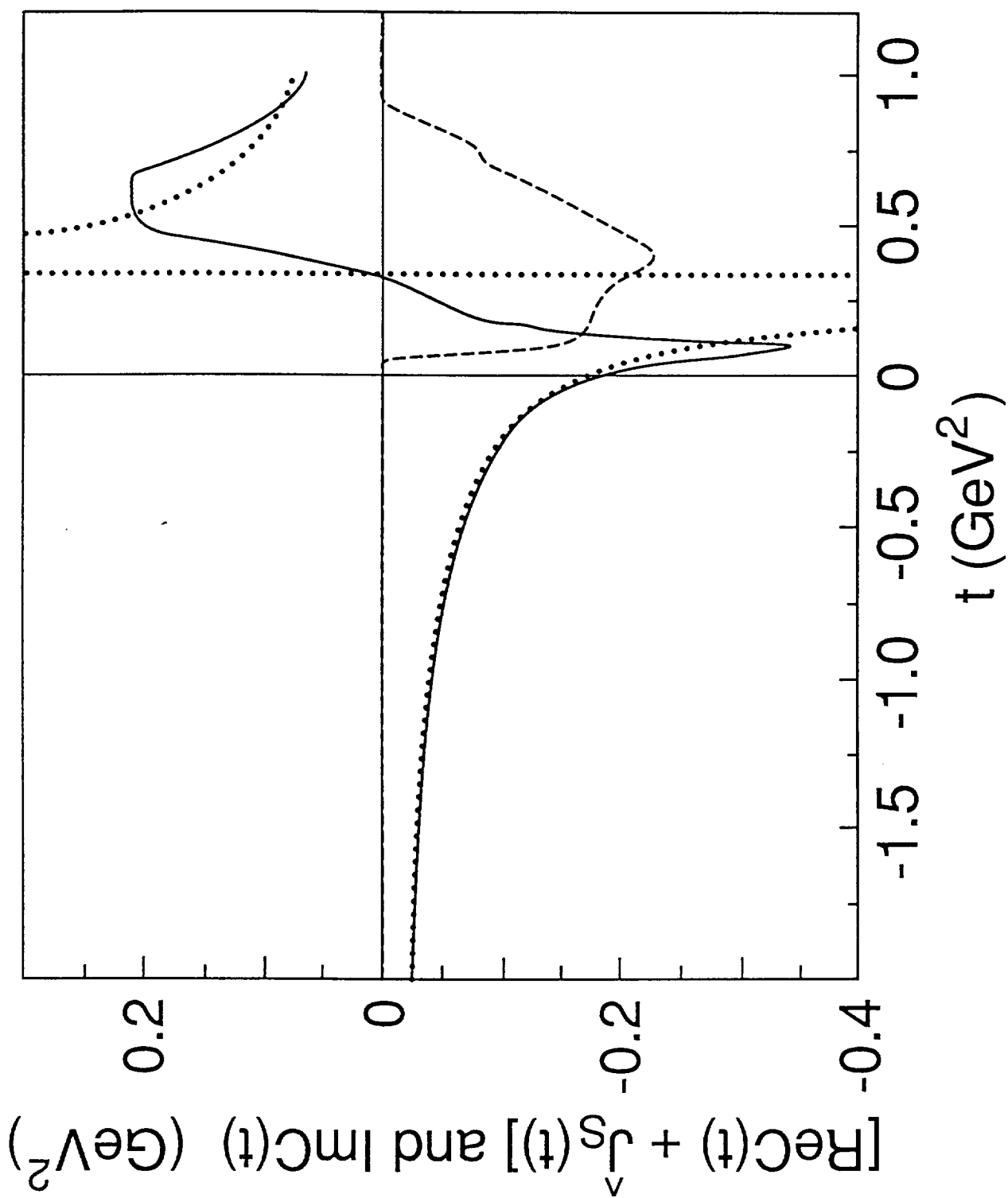


FIG. 6

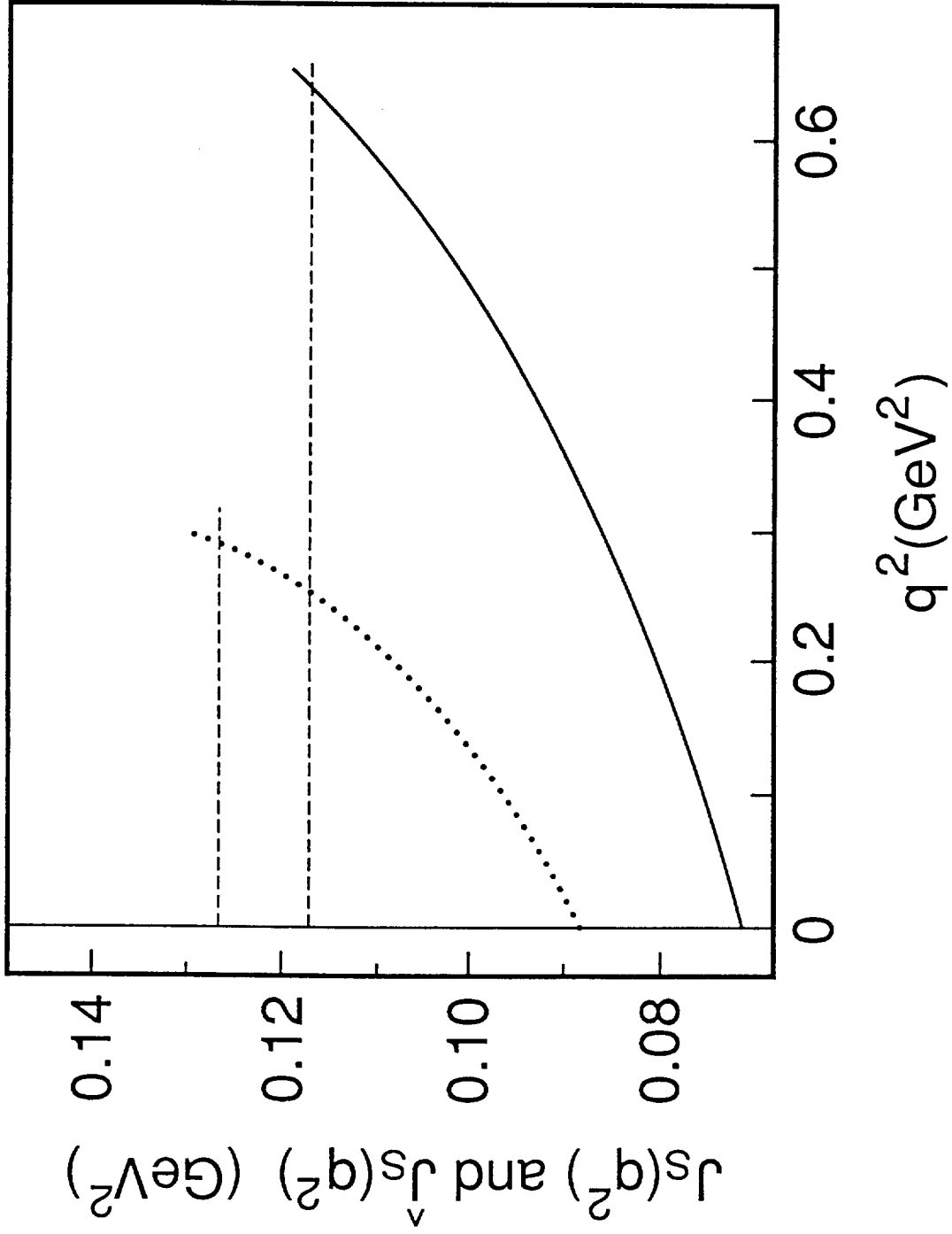


FIG. 7

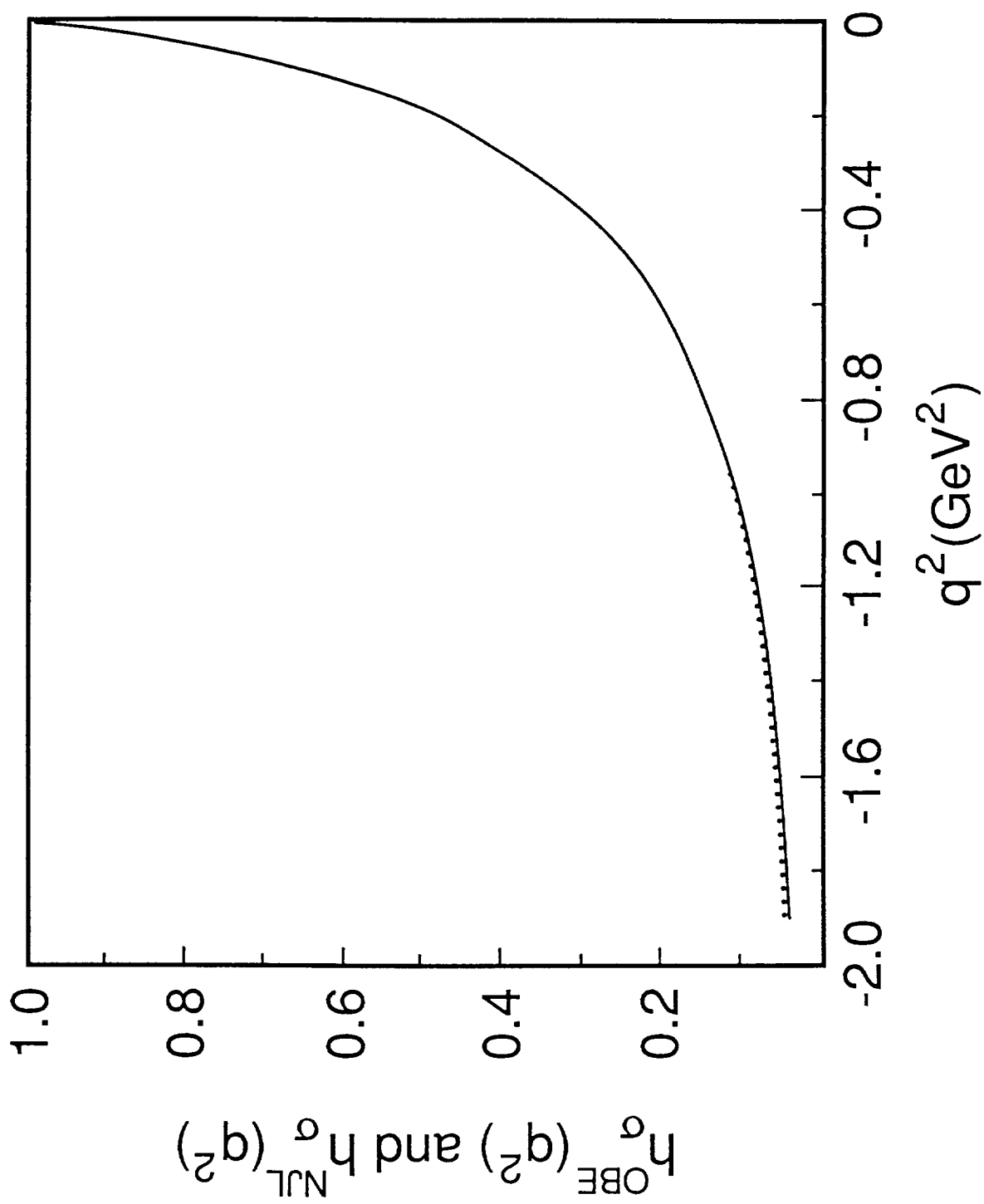
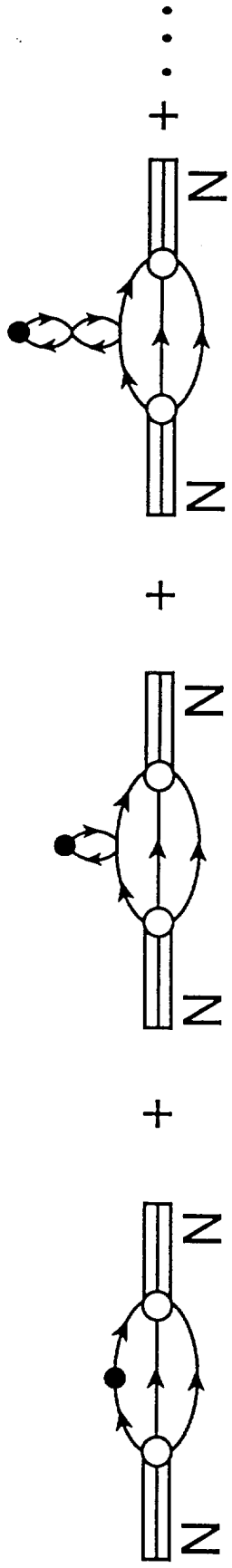
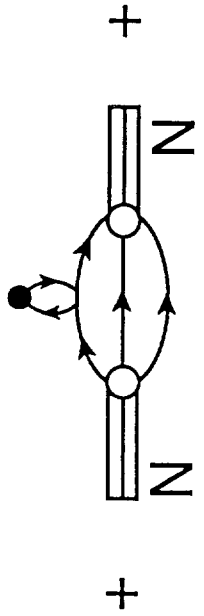


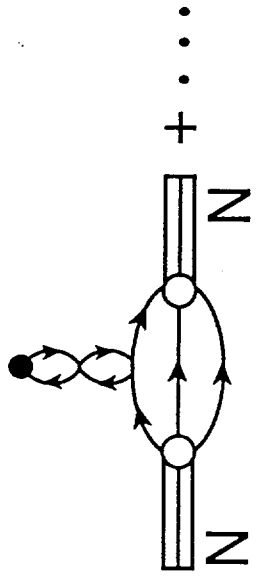
FIG. 8



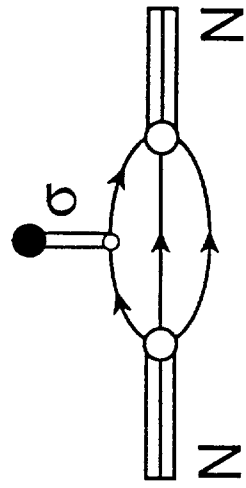
(a)



(b)



(c)



(d)

FIG. 9

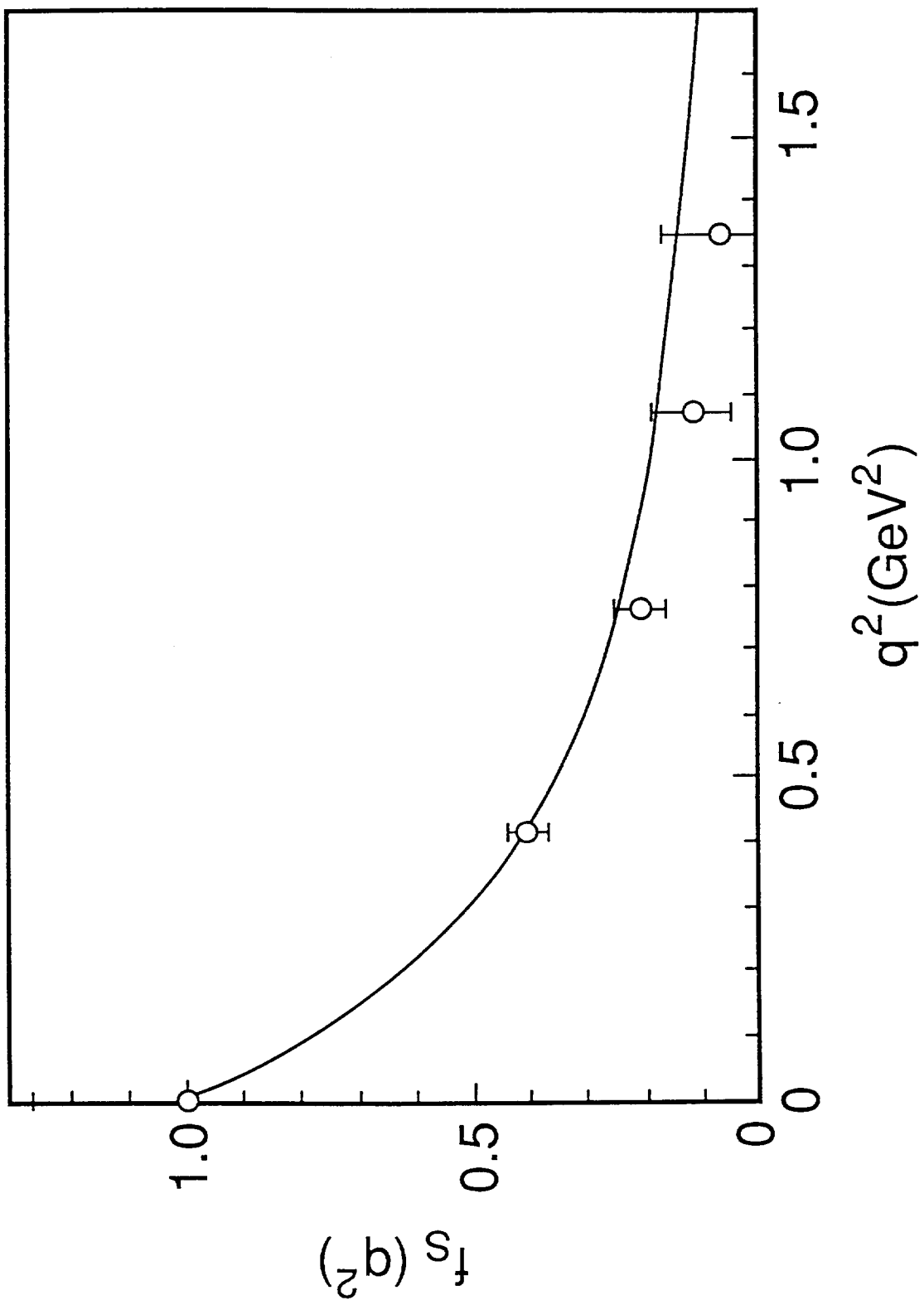


FIG. 10

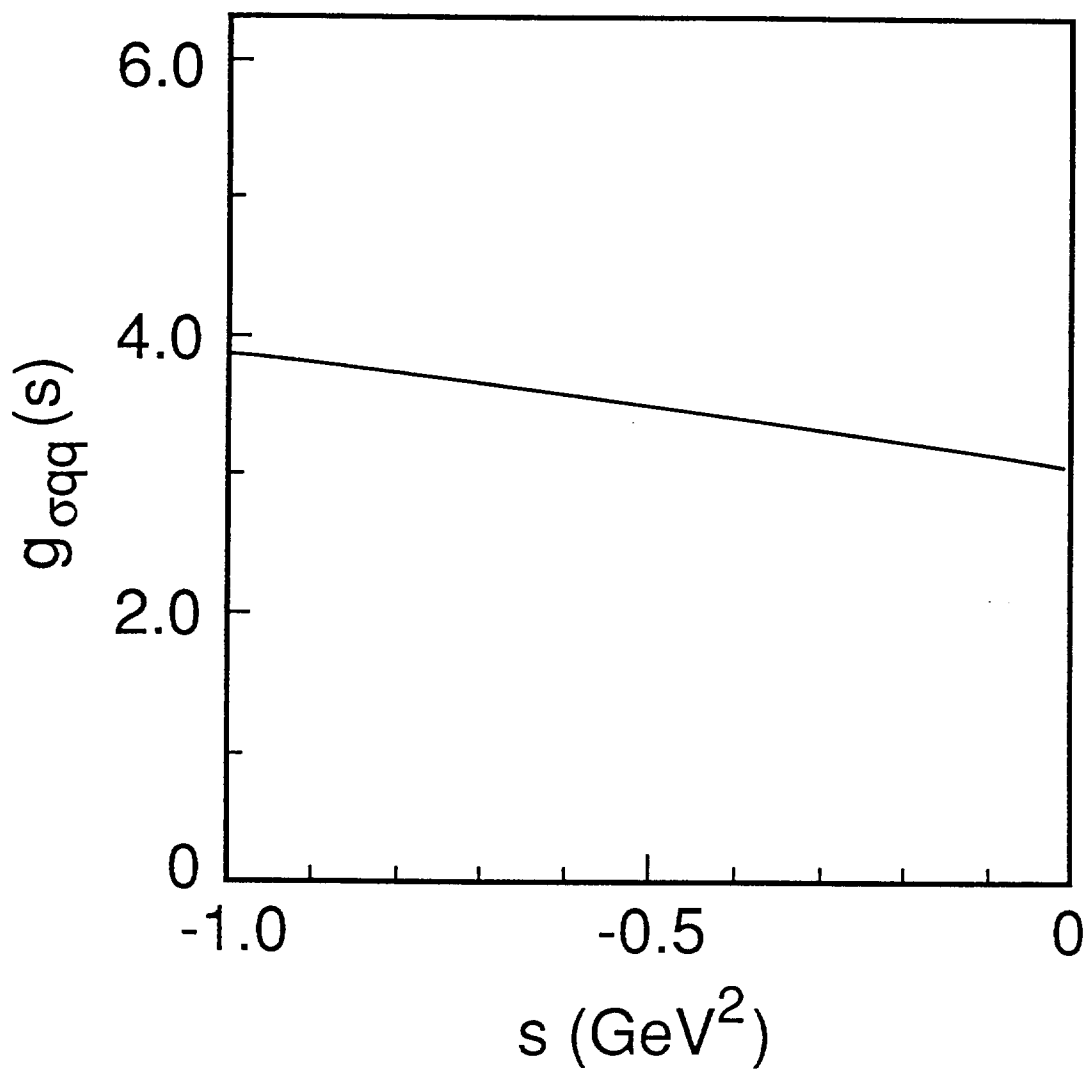


FIG. 11